Dynamic Simulation of Biodiesel Washing Column

Manuel L. Pinho
manuel.pinho@tecnico.ulisboa.pt

Instituto Superior Técnico, Lisboa, Portugal

November 2021

Abstract

This work focuses on developing a high fidelity dynamic model of a biodiesel washing column and the implementation of a multivariable control system. Its development was motivated by an increasing occurrence of problems in these columns when incorporating higher amounts of waste cooking oil and other low-quality fatty materials. This incorporation causes the formulations of raw oil to change significantly, requiring process flexibility and adequate control systems to maintain the product within strict quality standards and prevent operational problems. An overview of the biodiesel industry and production processes is first presented, with more detail in the homogeneous alkali process. The different liquid-liquid extraction columns are presented and the most used mathematical approaches to model these columns are briefly explained. The construction of the rate-based model of the column is shown (developed in gPROMS® ModelBuilder), accounting with mass transfer and hydrodynamics phenomena, such as holdup, flooding, and phase inversion. The model was validated against data from an industrial unit. A 2 $\times$ 2 control system was implemented in Simulink®, consisting of two PI controllers and two decouplers to minimise closed-loop interactions. The behaviour of the extraction column was simulated for the following scenarios: change in biodiesel composition; contamination in biodiesel inlet; and change in glycerol concentration in the washing water. The impact of these disturbances on the column hydrodynamics (e.g., the existence of flooding, phase inversion) and product quality was observed. Finally, the performance of the system in open-loop, closed-loop, and closed-loop with decouplers was compared.

Keywords: Biodiesel, Liquid-liquid extraction, Multivariable control, Rate-based model

1. Introduction

Biodiesel, fatty acid methyl esters (FAME), is a widely marketed biofuel in the transportation sector produced from the transesterification of vegetable oils, frying oils, animal fats, or from the esterification of fatty acids. It reduces carbon emissions, total hydrocarbon, and particulate matter by $15\,\%$ in a $20\,\%$ blend (B20) compared to diesel [8]. The biodiesel industry in Portugal has been steadily expanding with an average annual growth rate of $4.1\,\%$ [1].

Biodiesel production can be divided into three main processes: (i) raw material pretreatment; (ii) raw material conversion; and (iii) product purification. The pretreatment involves degumming, deacidification and water suspended particles, and polymers removal [25]. These contaminants lead to the formation of soaps, catalyst neutralization, and hinder phase separation of oil/glycerol. Following the pretreatment is the conversion process where biodiesel is produced through the transesterification of acylglycerides with methanol in the presence of a catalyst, producing glycerol as by-product. This catalyst can either be homogeneous or heterogeneous, and its nature acidic, alkaline or enzymatic [21]. The alkaline homogeneous catalysts (e.g., KOH, NaOH, $NaOCH_3$, $KOCH_3$) have high reaction rates, resulting in higher yields and shorter reaction times and so they are commonly used in industry. On the other hand, they are sensitive to raw material purity, particularly to low grade fats that contain higher concentrations of free fatty acids and water. A typical block diagram of the alkaline biodiesel production process is illustrated in Figure 1.

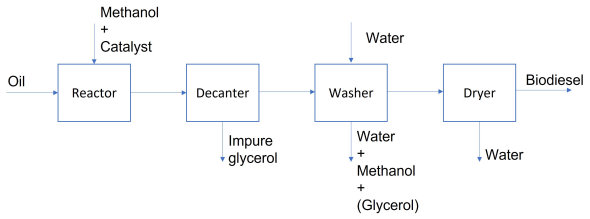

Figure 1: Block diagram of the alkaline biodiesel production process.

Finally, after the transesterification reaction, the biodiesel must be purified to reduce the concentration of glycerol, methanol and water. The post

reaction processing focuses on the recovery of esters from the reaction mixture and the necessary refining to meet the quality specifications ASTM D6751 or EN14214 [21]. The first step is usually the ester/glycerol separation, after which the majority of glycerol is removed and biodiesel washed. Water washing is an efficient method that produces biodiesel with high purity: water is added to the esters to eliminate the remaining glycerol, methanol, catalyst, and any remaining soaps [21]. This step can be achieved with a liquid-liquid extraction column. Lastly, the biodiesel needs to be dehydrated, usually accomplished with a dryer.

The cost of raw material is the major factor in the economic viability of biodiesel production, representing about $75\,\%$–$80\,\%$ of the total operating cost [9]. Regulations of the European Union stipulate limits to first-generation biodiesel and to crops cultivation for energy purposes to avoid the competition with the food market. In this context, the incorporation of waste cooking oils (UCO) can greatly reduce the total manufacturing cost of biodiesel, since it is 2.5 to 3.5 times cheaper than virgin vegetable oils [9]. Consequently, the amount of UCO used as raw material for biodiesel production in the European Union has been growing over the last years [13, 10]. This trend causes the formulations of raw oil to fluctuate significantly, requiring more process flexibility and adequate control systems to maintain the product within strict quality standards and to prevent operational problems.

Currently, the literature of process control in the biodiesel industry are focused on the transesterification reaction section and the biodiesel washing step is modelled with simplified models, e.g., [5, 4]. However, subtle changes in the oil composition (i.e., incomplete reaction, soaps, or fine solids in suspension) can promote the formation of stable emulsions in the washing column that need to be handled, before causing shutdowns and extra manufacturing costs. With the increasing tendency of incorporating lower-quality raw materials to make biodiesel, the problems related with the oil composition will have a significant impact on the column and will become more frequent. As such, the development of a detailed dynamic model of this unit is valuable and the design of a control system with good disturbance rejection capabilities is necessary and urgent.

The objectives of this work are the development of a highly detailed dynamic model of an industrial extraction column capable of capturing key physical phenomena occurring in this equipment unit; the validation of the extraction column model with industrial data; and lastly, the implementation of a robust control system to keep the product within quality standards, and to prevent operational problems. The remaining of the paper is structured as follows. section 2 presents the model development and Section 3 the model validation. The results regarding control design and tuning are detailed in Section 4, followed by final remarks in Section 5.

2. Model development

Liquid-liquid extraction equipment promotes the contact between two liquid phases to guarantee an efficient solute transfer [2]. This is accomplished by dispersing one liquid (the dispersed phase) into the other (the continuous phase), which increases the specific area for mass transfer. Liquid-liquid extraction columns are the most used and efficient equipment for biodiesel washing.

A thorough understanding of the extraction column requires an understanding of the different physicochemical mechanisms occurring in extraction, see Figure 2.

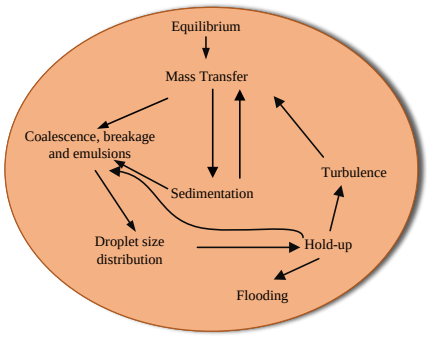

Figure 2: Scheme of the main phenomena related to extraction and their relations.

There are basically three approaches to model extractors: (i) equilibrium-based; (ii) rate-based; and (iii) population balance. In the first one, the column is described as a series of completely mixed stages to which mathematical equations are developed based on the principle of thermodynamic equilibrium, mass and energy conservation applied to each stage [16]. The rate-based models use mass and heat transfer phenomena across the interface to describe the compounds concentration profiles in each phase and the temperature profile along the column. It is assumed that all the resistance to mass and energy transfer is located adjacent to the phase boundary and each phase is completely mixed in each segment, with the dispersed phase treated as pseudo-homogeneous [20]. With this model, the hydrodynamics of the column can be described by a broad variety of correlations for the holdup, flooding, coalescence velocity, interfacial area and height. Finally, the population balance approach is based on a set of integro-partial differential equations to describe the behaviour of a population of particles and its environment from the behaviour of single particles in their local environments [3].

2.1. Dynamic model of biodiesel washing column

A simplified diagram of the packed column is illustrated in Figure 3. Here, the water, enters at the top of column, while biodiesel enters at the bottom. In this system biodiesel is the dispersed phase so its droplets rise through the column always in contact with the continuous-phase, water. The droplets build up and form the interface, where mass transfer occur.

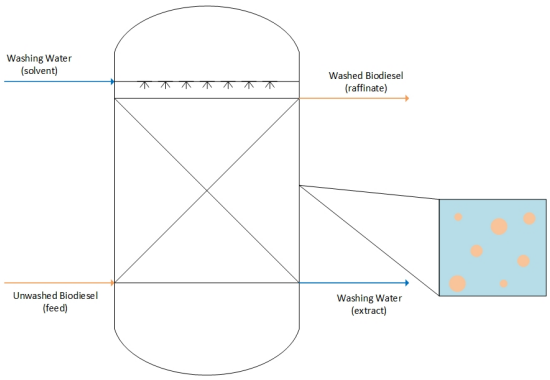

Figure 3: Simplified example of the liquid-liquid extraction for the system biodiesel/water with a section of the column.

The dynamic model of the extraction column implemented in this work assumes the system to behave as a pseudo-homogeneous dispersion because it is capable of describing the relevant phenomena of interest [6]. Preliminary simulations with the equilibrium approach revealed unsatisfactory results. The column is assumed to operate isothermally and so heat balances were not considered. In the sensitivity analysis the impact of temperature on the solubilities was investigated but these simulations were conducted at steady-state.

The general unsteady state mass balance equations for the continuous and dispersed phases are represented in Equations 1 and 2, respectively [16].

$$\frac{\partial(C_c\phi_c)}{\partial t} = V_c\frac{\partial(C_c)}{\partial z} + E_c\phi_c\frac{\partial^2(C_c)}{\partial z^2} - k_{od}a_I(C_d^* - C_d) \tag{1}$$

$$\frac{\partial(C_d\phi_d)}{\partial t} = -V_d\frac{\partial(C_d)}{\partial z} + E_d\phi_d\frac{\partial^2(C_d)}{\partial z^2} + k_{od}a_I(C_d^* - C_d) \tag{2}$$

where z is measured in the direction of flow of the dispersed phase; the subscripts c and d refer to the continuous and dispersed phases, respectively, V is the superficial phase velocity $(\mathrm{m/s})$, E is the axial dispersion coefficient $(\mathrm{m^2/s})$, a_I is the specific contact area $(\mathrm{m^2/m^3})$, ϕ_d is the volume fraction holdup, ϕ_c is $1-\phi_d$ and k_{od} is the overall mass transfer coefficient based on the dispersed phase $(\mathrm{m/s})$. Gayler and Pratt (1957) showed that backmixing of the dispersed phase does not occur [12]. Forward dispersion, however, is observed and happens due to differing droplet sizes and velocity but because of high coalescence and breakage rate in packed columns this is not as important as continuous phase backmixing [12]. Thus, $E_d = 0$. The boundary conditions for this system are:

$$z = 0 \quad C_d^{in}u_d^{in} = \phi_d V_d C_d \tag{3}$$

$$\frac{\partial(\phi_c V_c C_c)}{\partial z} = 0 \tag{4}$$

$$z = L \quad \frac{\partial(\phi_d V_d C_d)}{\partial z} = 0 \tag{5}$$

$$C_c^{in}u_c^{in} = \phi_c V_c C_c + E_c\frac{\partial(\phi_c C_c)}{\partial z} \tag{6}$$

These boundary conditions are the result from material balances across the system's boundaries and it is assumed that dispersion occurs only between $z = 0^+$ and $z = L^-$ [26] (L is the height of the column). The initial conditions are:

$$0 = V_c\frac{\partial(C_c)}{\partial z} + E_c\phi_c\frac{\partial^2(C_c)}{\partial z^2} - k_{od}a_I(C_d^* - C_d) \tag{7}$$

$$0 = -V_d\frac{\partial(C_d)}{\partial z} + E_d\phi_d\frac{\partial^2(C_d)}{\partial z^2} + k_{od}a_I(C_d^* - C_d) \tag{8}$$

For Equations 1 and 2, the volume fraction holdup was calculated with Equation (12) and the axial dispersion coefficient for the continuous phase was obtained with the Becker axial mixing model correlation for structured packed columns [11]. The overall mass-transfer coefficient was calculated with the following equation:

$$\frac{1}{k_{od}} = \frac{1}{k_d} + \frac{m_{dc}^{\mathsf{vol}}}{k_c} \tag{9}$$

where $m_{dc}^{\mathsf{vol}} = dC_d/dC_c$ is the slope of the equilibrium line in volumetric units, k_d and k_c are the dispersed- and continuous-phase film coefficients, respectively, and were calculated with Equations 10 (the Handlos and Baron model), and 11 for non-rigid drops in packing columns.

$$k_d = \frac{0.00375V_{\mathsf{slip}}}{1+\mu_d/\mu_c} \tag{10}$$

$$k_c = 0.698\left(\frac{\mathscr{D}_c}{d_p}\right)\left(\frac{d_p V_{\mathsf{slip}}\rho_c}{\mu_c}\right)^{0.5}\left(\frac{\mu_c}{\rho_c\mathscr{D}_c}\right)^{0.4}(1-\phi_d) \tag{11}$$

The diffusivity coefficient, $\mathscr{D}$ was estimated with the Wilke and Chang correlation [22]. V_{slip} is the slip velocity [11]. To calculate the density of the mixture, Kay's mixing rules were used to account with the molar weights and molar volumes

of biodiesel [18], the fraction of the acylglycerols [28], and the molar volumes of glycerol, water and methanol [19]. The impact of the polarity of components such as glycerol and methanol was not considered since the concentrations of these compounds in both phases are low. The GCVOL group contribution method was used to compute the biodiesel density [18] and a fragmented approach was used to estimate the fraction of acylglycerols [28]. The molar volumes of the remaining compounds (e.g., glycerol, methanol, water) were estimated with the Rackett equation [19]. Similarly, the dynamic viscosity of biodiesel is estimated with the Grunberg-Nissan model [7]. For the fatty species, the viscosity was calculated with the model of Ceriani et al. [7], while the viscosity of glycerol, water and methanol with the DIPPR liquid viscosity model [17]. Finally, the liquid-liquid interfacial tension of the system is computed using a local composition model by Jufu et al. [14].

2.2. Holdup and interface Level

Holdup, ϕ_D, in packed columns is known as the volume of the dispersed phase expressed as a fraction of the void space in the packed section and for a static extractor is calculated as follows [11]:

$$\phi_d = \frac{V_d[cos(\pi\frac{a_p d_p}{2}/4)]^{-2}}{\varepsilon[V_{so}\mathsf{exp}(\frac{-6\phi_d}{\pi}) - \frac{V_c}{\varepsilon}(1-\phi_d)]} \tag{12}$$

where the subscripts c and d are relative to the continuous and dispersed phases, respectively, V_{so} is the slip velocity at low dispersed-phase flow rate $(\mathrm{m/s})$, V is the liquid velocity $(\mathrm{m/s})$, a_p is the specific packing surface area $(\mathrm{m^2/m^3})$, d_p is the Sauter mean drop diameter and ε is the void fraction. The equations and conditions to calculate these variables are shown in Frank et al. [11]. The slip velocity (and the holdup, consequently) are dependent on H_{so} (Equation (13)), a measurement of coalescence velocity.

$$H_{so} = \left(\frac{4d_p^2 g\Delta\rho}{3\sigma}\right)\left(\frac{\mu_w}{\mu_c}\right)^{0,14} P^{0,149} \tag{13}$$

where μ is the liquid viscosity $(\mathrm{Pa\,s})$, μ_w is the reference viscosity of water $(\mathrm{Pa\,s})$, ρ is the liquid density $(\mathrm{kg/m^3})$, σ is the interfacial tension $(\mathrm{N/m})$, g is the gravitational acceleration of $9.1\,\mathrm{m^2\,s^{-1}}$ and P and H_{so} are dimensionless groups. The terminal velocity of a droplet, u_t, is given by:

$$u_t = \frac{\mu_c Re}{\rho_c d_p} \tag{14}$$

It is important to note that when H_{so} is higher than 59.3, the terminal velocity stops increasing with the diameter because of the deformation of the droplets. If the diameter continues to increase, the flow becomes more oscillatory and irregular. This phenomenon negatively impacts the movement of the droplet and promotes the formation of aggregates in the dispersion zone of the column, leading to backmixing and lower separation efficiencies. On the other hand, smaller droplets have a similar behaviour as rigid spheres ($H_{so} < 2$) with no internal circulation, which undermines the advantages of having a high interfacial area available for mass transfer. So, the ideal Sauter mean diameter of the droplets of the dispersed phase should be large enough to guarantee a decent terminal velocity, and small enough to ensure a high interfacial area for mass transfer. The equations to determine the Sauter mean diameter of the drop, d_p, for structured packing, and the interface level are shown in Frank et al. [11].

2.3. Flooding

To calculate the flooding percentage for each phase, Equation (15) was used for the continuous phase and Equation (16) for the dispersed phase.

$$\%Fl_C = \frac{V_c}{V_{cF}} \times 100 \tag{15}$$

$$\%Fl_D = \frac{V_d}{V_{dF}} \times 100 \tag{16}$$

The flooding velocity of the continuous phase, V_{cF}, was calculated from Frank et al. [11]. The dispersed phase flooding velocity, V_{dF}, was calculated with the equation from Mackowiak [15].

2.4. Solubility correlation

One crucial parameter that determines the extent to which the components in two liquid phases are distributed at equilibrium is the partition or distribution coefficient [23]. In practical terms, the miscibilities can be expressed as mass fractions, and using a modified Misek correlation [26] that accounts for the effect of temperature, T, Equation (17) is obtained:

$$\mathsf{ln}K_i = \mathsf{ln}\frac{w_i^{\mathsf{bd}}}{w_i^{\mathsf{aq}}} = a_i{}^M w_i^{\mathsf{aq}} + \frac{b_i^M}{T} - c_i^M \tag{17}$$

where K_i is the partition coefficient of component i for a mass fraction basis; a_i^M, b_i^M, and c_i^M are the parameters of the modified Misek correlation; variable w_i^{bd} is the mass fraction of component i in biodiesel, and w_i^{aq} is the mass fraction of component i in the aqueous phase. The parameters were estimated from solubility data gathered by an industrial partner and are listed in Table 1.

Table 1: Modified Misek model parameters estimated from the regression of solubility data.

Parameters	Glycerol	Methanol	Water	FAME
a_i^M	-113.29	32.48	1.34	-4.83
b_i^M	-968.25	364.96	1338.49	-7.71
c_i^M	0	3.30	11.06	0.54

3. Model validation and sensitivity analysis

Simulations at steady-state are performed and compared against data points retrieved at normal working conditions for model validation. Then, sensitivity analysis was conducted to investigate the effects of contamination, interface level, and liquid atomisation in the process. For brevity sake, only the impact in the glycerol concentration profiles is presented.

The effect of the solvent-to-feed ratio, S/F, at 45 ℃ for UCO in the solubility of glycerol was analysed. From this analysis, it was observed that the K_i of glycerol, methanol and FAME increases with S/F, which is not observed for the water. The effect of the temperature on the solubility of glycerol with $S/F = 13.5\,\%$ was also evaluated. Increasing the temperature will increase the solubility of glycerol, and methanol in water (K_i decreases), and decrease their solubility in biodiesel. The impact of the different oils in the solubility of the glycerol was also analysed. It is possible to conclude that the ester profiles have a small impact on the solubility of the solvents, hence these plots are not presented here.

Figure 4 illustrates the concentration profile of glycerol in biodiesel for different S/F at 45 ℃ where the unwashed and washed biodiesel from the experimental studies are represented with markers and are positioned in their values at the top and bottom of the column. Here, the increase in S/F has the same impact as observed above.

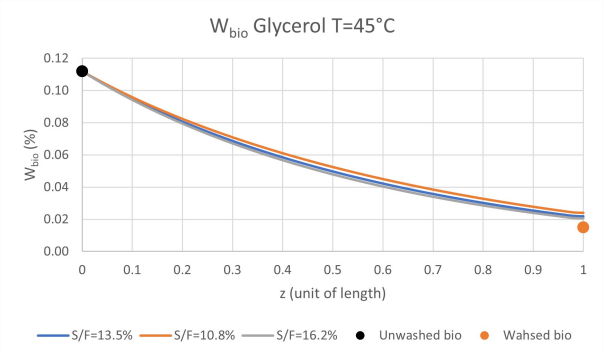

Figure 4: Glycerol concentration profile in biodiesel for different S/F compared with typical process values (markers).

The effect of temperature on the solubility of glycerol is shown in Figure 5. Increasing the temperature has the same effect as mentioned above. The relative errors for the composition of washed biodiesel are 46.1% for glycerol, 31.4% for methanol, 29.7% for water, and 0.2% for FAME. The model satisfactorily predicted the solubility of the solvents in biodiesel.

Finally, the impact of different ester concentration profiles in the solubility of glycerol in both phases was analysed. The different oils have

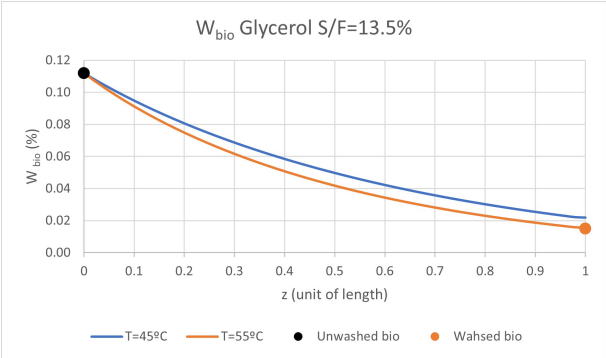

Figure 5: Glycerol concentration profile in biodiesel for different temperatures compared with typical process values (markers).

barely no effect on the solubility of glycerol in biodiesel and, even though there is some difference in the composition profile of glycerol in the aqueous phase, the washed biodiesel has approximately the same composition of glycerol. Thus, using different oils will not significantly impact the process, which was already verified industrially.

3.1. Sensitivity analysis

After validating the model, it is presented in this section the sensitivity analysis to evaluate the hydrodynamics of the column. Particularly: (i) the effect of contamination or incomplete reaction (small suspended particles or surfactants) - reflected through the interfacial tension; (ii) the effect of the interface level by changing the holdup, which is given by the dispersed phase to continuous phase ratio; (iii) the effect of liquid atomisation/agitation intensity, which is simulated by the droplet diameter; (iv) the effect of density of the dispersed phase. For this sensitivity analysis, the base conditions are 45 ℃, a solvent to feed ratio of 13.5 vol$\%$ and a biodiesel inlet mass flowrate of reference.

Figures 6 and 7 show the impact of density in the solubility of glycerol in biodiesel for different temperatures and solvent to feed ratios, respectively. It is observed that decreasing the density is beneficial since it decreases the solubility of glycerol and water in the biodiesel. As seen before, a higher temperature and solvent to feed ratio will increase the purity of the biodiesel.

The parameter H_{so} was presented above and is proportional to the coalescence velocity. The impact of interfacial tension, droplet diameter, temperature, and solvent to feed ratio on this parameter were analysed. It was observed that the solvent to feed ratio had no effect on H_{so}, so the plot will not be shown. The impact of liquid atomisation or agitation of biodiesel was modelled by changing the particle diameter (d_{32}), and is shown in Figure 8. Figure 9 shows the effect of the interfacial tension on H_{so} for different temperatures. Here,

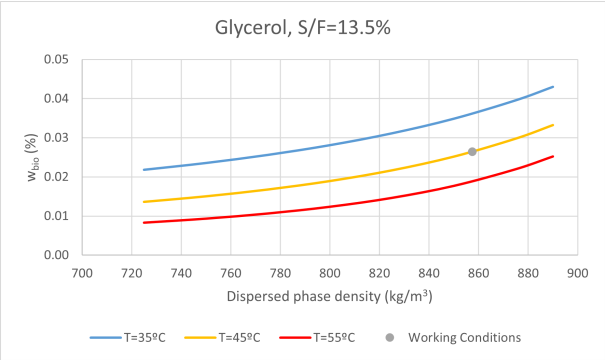

Figure 6: Impact of dispersed phase density in glycerol solubility in biodiesel for different temperatures with a biodiesel inlet mass flowrate of reference.

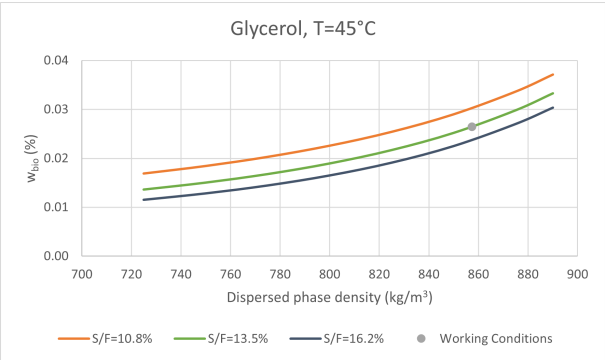

Figure 7: Impact of dispersed phase density in glycerol solubility in biodiesel for different solvent to feed ratios with a biodiesel inlet mass flowrate of reference.

it is possible to see that this parameter increases significantly with the diameter of the particles and also with the interfacial tension.

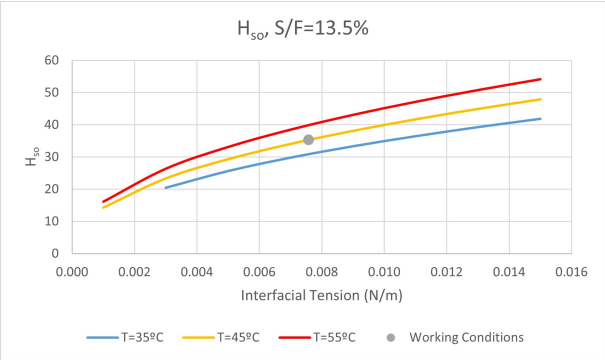

Figure 8: Impact of the particle diameter in dispersed phase (biodiesel) coalescence velocity for different temperatures with a biodiesel inlet mass flowrate of reference.

If the droplets are too small ($d_{32} \approx 1.0\,\mathrm{mm}$) they will have a similar behaviour as rigid spheres and will hinder the coalescence phenomenon [12]. This can promote the entrainment of washing water that will exit the column through the dispersed phase outlet. On the other hand, for $d_{32} > 3.5\,\mathrm{mm}$ $H_{so} > 53$, which suggests insufficient droplet rise that may lead to a inefficient extraction [12]. Higher values of H_{so} will also promote phase inversion

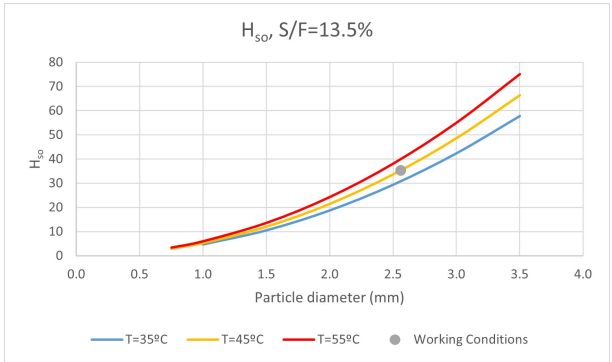

Figure 9: Impact of interfacial tension in dispersed phase (biodiesel) coalescence velocity for different temperatures with a biodiesel inlet mass flowrate of reference.

since there is early coalescence of the particles. Lastly, the effect of temperature is significant, however, manipulating this variable to change the convergence velocity of the droplets will not be efficient.

For the impact of interfacial tension on H_{so}, higher values of interfacial tension will lead to insufficient droplet rise, however, contamination usually decreases this value and not the opposite. In case of low interfacial values, this will promote droplet breakdown, since there is not enough tension to keep the droplets and, consequently, the interface level will decrease. This decrease in the interface level will increase the probability of phase inversion to occur, which can be seen in Figure 10.

Finally, the effects of the interfacial tension and the interface level on the hydrodynamics of the column were analysed and are shown in Figure 10 ($S/F = 13.5\,\%$ and $T = 45\,$℃). The same effects were tested for the system with the following conditions: (i) $S/F = 16.2\,\%$ and $T = 45\,$℃, and (ii) $S/F = 16.2\,\%$, $T = 50\,$℃ and interfacial tension of $0.001\,\mathrm{N\,m^{-1}}$. In this plot, the vertical black line represents the value of the interface level calculated by the model for the working conditions; and the horizontal dashed line corresponds to the maximum recommended percentage of flooding [11]. It is also important to note that the interfacial tension of the system is usually around $0.008\,\mathrm{N\,m^{-1}}$.

Figure 10 provides two different information: (i) which phase is more probable to be dispersed, according to the interface level; (ii) for a given interfacial tension, it returns the flooding percentage of the continuous phase (- - -) and dispersed phase (—) calculated with Equations 15 and 16.

Analysing Figure 10, it is possible to see that the interface level should be lower than $0.70\,\mathrm{length\ units}$ so the flooding percentage of either phase is below $60\,\%$ and higher than $0.63\,\mathrm{length\ units}$ to avoid phase inversion. From this figure, it is also observable that with contamination, the flooding percentages increase. The

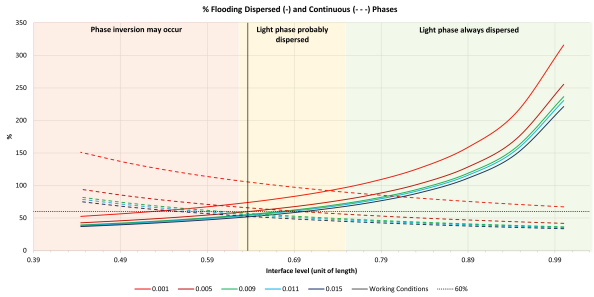

Figure 10: Impact of interfacial tension in flooding of both phases with an indicator of phase inversion with solvent to feed ratio of $13.5\,\%$, $45\,^{\circ}\mathrm{C}$ and biodiesel inlet mass flowrate of reference.

working conditions demonstrated that the current interface level corresponds to a flooding percentage within the recommend values in most situations. However, for low interfacial tensions, close to $0.001\,\mathrm{N\,m^{-1}}$, both phases exceed this value, which is aggravated by increasing S/F (concluded from analysis (1.)). That is, a higher contamination will increase the flooding percentage of both phases, which is not reversible by changing the solvent to feed ratio, nor the interface level for a given biodiesel inlet flowrate. The impact of the biodiesel inlet flowrate on these variables was studied with the conditions mentioned in (2.). From this analysis, it was possible to conclude that by reducing the inlet flowrate of biodiesel to $64\,\%$ of the reference value, it is possible to reduce the flooding percentage of the continuous phase to roughly $60\,\%$. Ideally, the interface level should be around $16\,\%$ higher.

That being said, the suggested operating conditions are temperature at $50\,^{\circ}\mathrm{C}$ and S/F of $16.2\,\mathrm{vol}\%$. In case of contamination, the biodiesel inlet flowrate should be lowered to 2/3 of its original value, the interface level should be increased in $16\,\%$ keeping the S/F at $16.2\,\mathrm{vol}\%$.

4. Control of the extraction column

To simplify the notation, in this section, all input/output variables will be presented as deviation variables (so their nominal value is 0). For this section, the analysis was conducted with UCO, at $45\,^{\circ}\mathrm{C}$ and a S/F of $13.5\,\mathrm{vol}\%$. The impact of the temperature on the system was not analysed here, the temperature is assumed to be constant.

Regarding extraction columns, most control models focus on the interface level between the two phases inside the column and outlet concentrations control [26]. If this level is not adequately stabilised, the dispersed layer can flood, causing the loss of solvent and product [26]. The manipulated variables (MV) used to control the holdup and outlet concentrations are usually the dispersed-phase flow rate, the continuous-phase feed/effluent flow rate and the rotor speed.

4.1. Open-loop testing and system linearisation

Open-loop testing is a crucial procedure to analyse how the system reacts to certain disturbances. Having already an accurate model, input variables such as inlet flowrate, temperature and composition, are subject to intentional changes to observe how they will impact the output variables without the influence of a controller.

The impact of disturbances in input variables related to the biodiesel formulation, such as interfacial tension, density and viscosity, and inlet glycerol composition (that reflects a poor phase separation) on the glycerol composition (wt$\%$) of the biodiesel outlet stream, flooding percentage of both phases, holdup and in the phase inversion parameter (χ) were studied. It was also analysed the effect of step disturbances on the inlet and outlet mass flowrates of biodiesel and water on the output variables mentioned above.

From the step disturbances applied to the input variables related to the biodiesel formulation, the ones that had a more severe impact on the output variables were the interfacial tension, density, and glycerol composition of the biodiesel inlet stream. For this reason and for the sake of brevity, the viscosity and the glycerol composition of the washing water will not be further analysed here.

It was observed that a disturbance in the interfacial tension has a significant impact on the flooding percentages, but not in the other variables. However, it was expected to see a decrease in holdup with the interfacial tension, since there will be less tension to form the droplets. This happens because the model does not incorporate population balance equations. For the density, a disturbance in this variable had a significant impact on the flooding percentage of the continuous phase, and also on the holdup and χ. Finally, the disturbances on the biodiesel glycerol inlet composition had a severe impact on the composition of the washed biodiesel.

For the disturbances on the mass flowrates, it was observed that a variation on the inlet or outlet flowrate had the exact same effect on the system, which was observed for both phases. This happens due to the limitations of the model, the holdup is not considered to vary with time. Overall, a disturbance in the biodiesel or water mass flowrates has a significant impact on the flooding percentages, holdup and χ, and a small impact on the glycerol composition of biodiesel.

In order to proceed with the development of a control system in MATLAB® it was necessary to linearise the system, which was achieved with the *System Identification* toolbox from MATLAB®. All

transfer functions had a fit to estimation data higher than $94\,\%$.

4.2. Variable pairing

To analyse this multivariable process control problem, Bristol's Relative Gain Array (RGA) and Singular Value Analysis (SVA) methods were used [24]. Since manipulating both inlet and outlet flowrates for biodiesel and water would lead to a over-specified system, only the outlet streams will be used for control purposes. Weinstein et al. [26] demonstrated that manipulating the outlet instead of the inlet flowrate would lead to a more smooth behaviour of the system. Consequently, there can only exist two controlled variables (CV): the mass fraction of glycerol in biodiesel was always analysed with one more of the mentioned variables except χ since it is the least directly dependent on the level of the interface.

From the RGA and SVA methods, the pairings: **glycerol outlet composition — water outlet flowrate**, and **holdup — biodiesel outlet flowrate** are the most recommended. The other possible pairings had singular steady-state gain matrices, which means they are ill-conditioned.

The control scheme is illustrated in Figure 11. The nomenclature used in Figure 11 will be used to refer to the controllers in the next subsection.

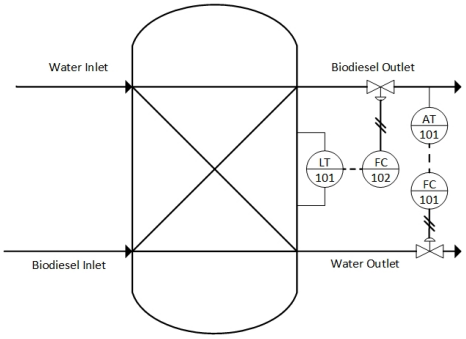

Figure 11: Control scheme for the biodiesel extraction column.

4.3. Controller tuning

Knowing which variables to pair, it is now necessary to tune the controllers. The tested controllers were evaluated based on integral error criterion in set-point tracking and disturbance rejection. The three most used integral error criteria are: integral of the squared error (ISE), integral of the absolute value of the error (IAE), and integral of the time-weighted absolute error (ITAE). Here, the IAE was the deciding factor to select the controllers, which has a criterion that penalises both large errors and errors that persist for a long time period.

The control system was also analysed in terms or relative stability with the concepts of Gain Margin (GM) and Phase Margin (PM), these values indicate how close the system is to become unstable [24]. All controllers were tuned in Mathematica® with Ziegler-Nichols (ZN), Internal Model Control (IMC), and Cohen-Coon (CC) tuning techniques available in the solver. Saturation was added to the MV, $-10\,\%$ to $10\,\%$ for biodiesel mass flowrate and $-20\,\%$ to $20\,\%$ for water mass flowrate. For this process, set-point changes are not expected, so only the results for disturbance rejection are shown.

Starting with the FC101 controller, the ZN and IMC (Skogestad) tuning methods were tested. These methods and the tuning procedures are explained in Seborg et al. [24]. The controller settings for the different tuning methods are presented in Table 2 with the values of GM and PM. The controller is in parallel and the derivative mode has a filter N.

Table 2: Controller settings for the controller FC101 according to ZN and IMC tuning methods and Gain and Phase Margins.

Tuning Method		ZN		IMC	
Controller mode		PI	PID	PI	PID
Controller Settings	K_P	-2.05E06	-2.73E06	-2.24E06	-1.07E09
	K_I	-7.21E07	-1.60E08	-6.36E07	-1.41E11
	K_D	-	-1.16E04	-	-8.08E05
	N	-	100	-	100000
Relative Stability	GM	68	1392	67	2
	PM (°)	34	23	37	47

For the disturbance rejection, a disturbance of $-80\,\%$ in the interfacial tension was applied to the system. The PI controller tuned with IMC has the smallest value of IAE, and so it was chosen.

Similarly to FC101, the controller FC102 was also tuned with two different methods. Both ZN and IMC tuning approaches were tested, however, the IMC tuning technique failed to return a viable controller. So, the CC tuning method was used instead of IMC. This method is explained in Woolf [27]. The controller settings and relative stability margins are shown in Table 3. Analysing this table, and taking the IAE criterion as the deciding factor, the PI controller tuned with CC rules has a slightly better performance when compared with the other ones. Hence, this was the chosen controller settings.

Table 3: Controller settings for the controller FC102 according to ZN and CC tuning methods and Gain and Phase Margins.

Tuning Method		ZN		CC	
Controller mode		PI	PID	PI	PID
Controller Settings	K_P	3.02E04	4.03E04	5.76E04	5.34E04
	K_I	1.64E06	3.65E06	9.21E06	5.18E06
	K_D	-	111	-	91.7
	N	-	100	-	1000
Relative Stability	GM	∞	∞	∞	∞
	PM (°)	156	∞	125	∞

All the controllers had the same value of IAE, so the PI controller tuned with the CC method was chosen because it has the smallest value for ITAE.

Two decouplers were added to minimise the interaction between the closed-loops. These were tuned according to procedures showed in Seborg

et al. [24]. However, analysing the transfer function of one the decouplers, it was identified a real right-half plane pole, which makes it unstable. So, static decouplers were used instead.

Having the multiloop with decouplers, it is interesting to evaluate if and how the system benefited from the addition of the closed-loops and decouplers. The response of the system in open-loop, closed-loop, and closed-loop with static decouplers to disturbances in interfacial tension, biodiesel density and feed glycerol composition are presented in Figures 12 to 14. The response of the MV is not shown here.

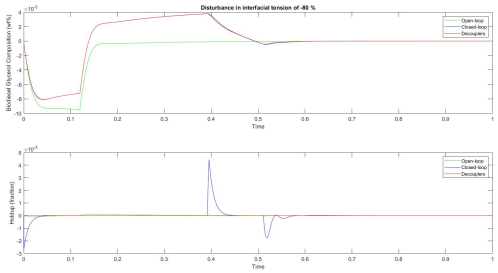

Figure 12: Evolution of the controlled variables: biodiesel glycerol composition (wt%) and holdup fraction to a disturbance in interfacial tension of $-80\,\%$.

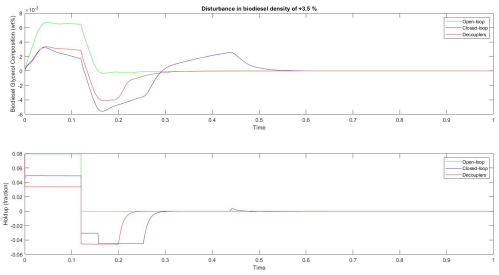

Figure 13: Evolution of the controlled variables: biodiesel glycerol composition (wt%) and holdup fraction to a disturbance in biodiesel density of $3.5\,\%$.

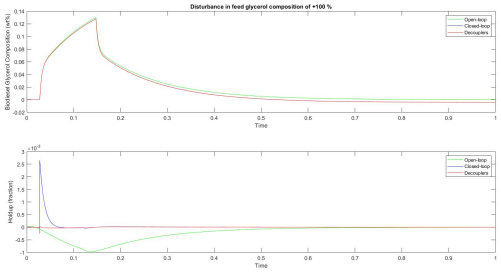

Figure 14: Evolution of the controlled variables: biodiesel glycerol composition (wt%) and holdup fraction to a disturbance in feed glycerol mass composition of $100\,\%$.

It is observed that the addition of decouplers to the control system was beneficial because, for set-point tracking, it was able to reduce settling-time, excessive oscillation and overshoots, and even reducing the duration of the actuator saturation. For disturbance rejection, the control of holdup greatly improved with the reduction of settling-time and lower overshoots; the control of biodiesel glycerol composition was not ideal due to an increase in oscillation, however the overshoots were minimised. Additionally, it was also observable that the closed-loop interactions were reduced by adding decouplers, and that they were successful in reducing excessive controller action.

5. Conclusions and future work

The present work focused on the development of a dynamic model of a biodiesel washing column which was motivated by a real problem in a biodiesel production plant. The usage of biodiesel from virgin oils is expensive so the incorporation of UCO has been growing in the last decade and is expected to keep this tendency. This alternative is economically and environmentally advantageous, however, the contamination present in these used oils present a challenge in the production of biodiesel, due to their quality, and quantity of impurities. The development of a dynamic model for the column helps to identify and avoid certain problems related to these impurities.

A dynamic rate-based model for the liquid-liquid extraction column was build, where mass transfer phenomena, hydrodynamics and biodiesel properties were estimated. The model was validated with industrial data provided by an industrial partner and the model accurately predicted the solubility of the solutes in the washed biodiesel. The effects of working conditions on the system were tested and are in accordance with the real plant. A sensitivity analysis was performed to evaluate the impact of the presence of impurities or different types of oils might have on the performance of the column. Additionally, other operating variables were also analysed such as the interface level, and the glycerol inlet composition. It was observed that at $50\ ^{\circ}\mathrm{C}$ and for a solvent to feed ratio of $16.2\,\mathrm{vol}\%$ the column had a better performance. In case of contamination, an approach to manipulate the working conditions was suggested in order to avoid flooding and phase inversion.

Finally, the system was further analysed in order to implement a 2 $\times$ 2 control scheme. The best suggested pairing was Glycerol outlet composition in biodiesel-water outlet flowrate, and holdup-biodiesel outlet flowrate. The controllers were then tuned with the IMC and CC methods, respectively. The addition of static decouplers was successful in minimising strong loop interactions. Overall, the control system has a good performance for set-point tracking and disturbance rejection.

The development of a dynamic model of a liquid-

liquid extraction column for a biodiesel/water system is innovative, more so with an implemented control system. It was not possible to develop a drop population balance model for this column due to lack of time, however, the development of this extremely detailed model could help surpass some of the observed limitations in the rate-based model. Furthermore, the implementation of a Model Predictive Control scheme would be highly interesting and undoubtedly useful to have a process running under the optimal working conditions.

References

[1] International Energy Data, Monthly Update. https://knoema.com/EIAINTL2018May/international-energy-data-monthly-update#, Accessed in 05-08-2021.

[2] E. G. Azevedo and A. M. Alves. *Engenharia de Processos de Separação*. 3ª edition, 2017.

[3] H. J. Bart, H. Jildeh, and M. Attarakih. Population Balances for Extraction Column Simulations—An Overview. *Solvent Extraction and Ion Exchange*, 38(1):14–65, 2020.

[4] A. S. Brásio, A. Romanenko, N. C. Fernandes, and L. O. Santos. First principle modeling and predictive control of a continuous biodiesel plant. *Journal of Process Control*, 47:11–21, 2016.

[5] A. S. Brásio, A. Romanenko, J. Leal, L. O. Santos, and N. C. Fernandes. Nonlinear model predictive control of biodiesel production via transesterification of used vegetable oils. *Journal of Process Control*, 23(10):1471–1479, 2013.

[6] A. C. G. Braz. *Profitability Increase of a Formaldehyde Production Plant*. PhD thesis, Instituto Superior Técnico, 2019.

[7] R. Ceriani, C. B. Gonçalves, and J. A. Coutinho. Prediction of viscosities of fatty compounds and biodiesel by group contribution. *Energy and Fuels*, 25(8):3712–3717, 2011.

[8] S. Chattopadhyay and R. Sen. Fuel properties, Engine performance and environmental benefits of biodiesel produced by a green process. *Applied Energy*, 105:319–326, 2013.

[9] A. Demirbas. Political, economic and environmental impacts of biofuels: A review. *Applied Energy*, 86(1):108–117, 2009.

[10] M. Ellen Smith, B. Flach, K. Bendz, and S. Lieberz. Biofuels Annual. Technical report, United States Department of Agriculture, 2012.

[11] T. C. Frank, L. Dahuron, B. S. Holden, D. Prince, William, A. F. Seibert, and L. C. Wilson. Liquid-Liquid Extraction and Other Liquid-Liquid Extraction Operations and Equipment. In *Perry's Chemical Engineers' Handbook*, number 11, pages 15–1 – 15–105. 2008.

[12] J. C. Godfrey and M. J. Slater. *Liquid-Liquid Extraction Equipment*. 1994.

[13] A. v. Grinsven, E. v. d. Toorn, R. v. d. Veen, and B. Kampman. Used Cooking Oil (UCO) as biofuel feedstock in the EU. Technical report, 2020.

[14] F. Jufu, L. Buqiang, and W. Zihao. Estimation of Fluid-fluid Interfacial Tensions of Multicomponent Mixtures. *Chemical Engineering Science*, 41(10):2673–2679, 1986.

[15] J. Mackowiak. *Fluid Dynamics of Packed Columns*. Springer, 1 edition, 2010.

[16] S. Mohanty. Modeling of liquid-liquid extraction column: A review. *Reviews in Chemical Engineering*, 16(3):199 – 248, 2000.

[17] A. Plus, A. Properties, A. E. Suite, A. Technology, T. C. Park, and O. Systems. Part Number : Aspen Physical Property System 11 . 1 September 2001. *Engineering*, pages 2–18, 2001.

[18] M. J. Pratas, S. V. Freitas, M. B. Oliveira, S. C. Monteiro, Á. S. Lima, and J. A. Coutinho. Biodiesel density: Experimental measurements and prediction models. *Energy and Fuels*, 25(5):2333–2340, 2011.

[19] H. G. Rackett. Equation of State for Saturated Liquids. *Journal of Chemical and Engineering Data*, 15(4):514–517, 1970.

[20] Ramesh K., Aziz N., Abd Shukor S.R., and Ramasamy M. Dynamic Rate-Based and Equilibrium Model Approaches for Continuous Tray Distillation Column. *Journal of Applied Sciences Research*, 3(12):2030–2041, 2007.

[21] M. Ramos, A. P. S. Dias, J. F. Puna, J. Gomes, and J. C. Bordado. Biodiesel Production Processes and Sustainable Raw Materials. *energies*, 4408(12):1–30, 2019.

[22] R. C. Reid, T. K. Sherwood, and R. E. Street. *The Properties of Gases and Liquids*. 4th edition, 1959.

[23] J. D. Seader, E. J. Henley, and D. K. Roper. *Separation Process Principles*. 4 edition, 2016.

[24] D. Seborg, T. Edgar, D. Mellicamp, and F. Doyle III. *Process Dynamics and Control*. 3 edition, 2011.

[25] A. Tafesh and S. Basheer. Pretreatment Methods in Biodiesel Production Processes. In *Pretreatment Techniques for Biofuels and Biorefineries*, chapter 18. Springer Berlin Heidelberg, 2013.

[26] O. Weinstein, R. Semiat, and D. R. Lewin. Modeling, simulation and control of liquid-liquid extraction columns. *Chemical Engineering Science*, 53(2):325–339, 1998.

[27] P. Woolf. 9.3: Pid tuning via classical methods - engineering libretexts. https://eng.libretexts.org/Bookshelves/Industrial_and_Systems_Engineering/Book%3A_Chemical_Process_Dynamics_and_Controls_(Woolf)/09%3A_Proportional-Integral-Derivative_(PID)_Control/9.03%3A_PID_Tuning_via_Classical_Methods, Accessed in 14-10-2021.

[28] L. Zong, S. Ramanathan, and C. C. Chen. Erratum: Fragment-based approach for estimating thermophysical properties of fats and vegetable oils for modeling biodiesel production processes. *Industrial and Engineering Chemistry Research*, 49(6):3022–3023, 2010.